

U.S. DEPARTMENT OF COMMERCE  
National Technical Information Service

AD-A025 334

SURFACE CHARACTERIZATION OF TITANIUM AND  
TITANIUM ALLOYS

PART I: EFFECT ON TITANIUM - 6 ALUMINUM -  
4 VANADIUM ALLOY OF COMMERCIAL TREATMENTS

AIR FORCE MATERIALS LABORATORY

MARCH 1976

166065

AFML-TR-76-29  
PART I

AD A 025334

**SURFACE CHARACTERIZATION OF TITANIUM  
ALLOYS PART I: EFFECT ON TITANIUM -  
6 ALUMINUM - 4 VANADIUM ALLOY OF  
COMMERCIAL TREATMENTS**

*MECHANICS AND SURFACE INTERACTIONS BRANCH  
NONMETALLIC MATERIALS DIVISION*

MARCH 1976

TECHNICAL REPORT AFML-TR-76-29, PART I  
FINAL REPORT FOR PERIOD JUNE 1975 - JANUARY 1976

Approved for public release; distribution unlimited

REPRODUCED BY  
NATIONAL TECHNICAL  
INFORMATION SERVICE  
U. S. DEPARTMENT OF COMMERCE  
SPRINGFIELD, VA. 22161

AIR FORCE MATERIALS LABORATORY  
AIR FORCE WRIGHT AERONAUTICAL LABORATORIES  
Air Force Systems Command  
Wright-Patterson Air Force Base, Ohio 45433



NOTICE

When Government drawings, specifications, or other data are used for any purpose other than in connection with a definitely related Government procurement operation, the United States Government thereby incurs no responsibility nor any obligation whatsoever; and the fact that the government may have formulated, furnished, or in any way supplied the said drawings, specifications, or other data, is not to be regarded by implication or otherwise as in any manner licensing the holder or any other person or corporation, or conveying any rights or permission to manufacture, use, or sell any patented invention that may in any way be related thereto.

This report has been reviewed by the Information (IO) and is releasable to the National Technical Information Service (NTIS). At NTIS, it will be available to the general public, including foreign nations.

This technical report has been reviewed and is approved for publication.

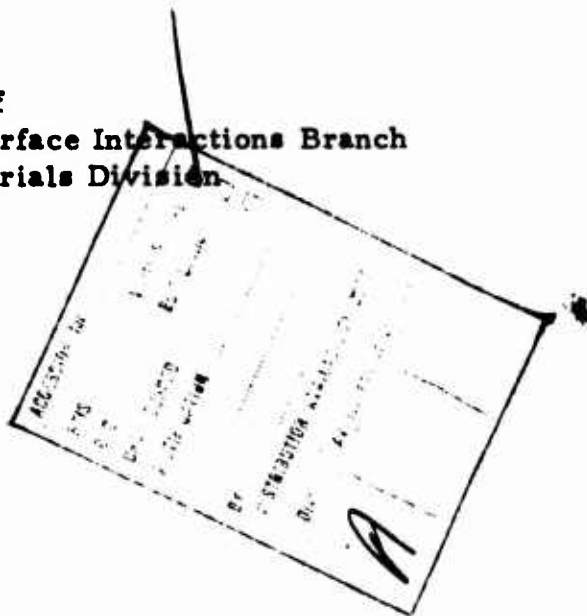


W.L. BAUN  
Project Monitor

FOR THE DIRECTOR



S.W. TSAI, Chief  
Mechanics and Surface Interactions Branch  
Nonmetallic Materials Division



Copies of this report should not be returned unless return is required by security considerations, contractual obligations, or notice on a specific document.

## FOREWORD

This technical report was prepared by William L. Baun, Mechanics and Surface Interactions Branch, Nonmetallic Materials Division, Air Force Materials Laboratory (AFML/MBM), Wright-Patterson Air Force Base, Ohio. The work was initiated under Project 7340, "Nonmetallic and Composite Materials" and was administered by The Air Force Materials Laboratory, Air Force Systems Command, Wright-Patterson Air Force Base, Ohio.

This report covers work conducted inhouse during the period June 1975 through January 1976. The report was released by the author in January 1976.

The author wishes to acknowledge the technical assistance of N. T. McDevitt, William Lampert, E. A. Arvay and H. S. Schwartz of the Air Force Materials Laboratory and of J. S. Solomon, R. Harmer and W. Moddeman of the University of Dayton Research Institute.

TABLE OF CONTENTS

SECTION	<u>PAGE</u>
I. INTRODUCTION	1
II. EXPERIMENTAL	3
III. SUMMARY OF EARLIER WORK	7
IV. RESULTS AND DISCUSSION	9
A. Ti-6Al-4V Alloy	
B. Effect of Surface Treatments	
1. As Received	
2. Alkaline Clean	
3. Alkaline Etch	
4. Phosphate-Fluoride	
5. Pasa-Jell 107	
6. VAST	
V. CONCLUSIONS	13
REFERENCES	14
APPENDIX A - Positions of Ion Scattering Peaks (E/E <sub>0</sub> ) for Z=1-50	15
APPENDIX B - Relative Abundance of Naturally Occurring Isotopes, Z=1-44	17
APPENDIX C - X-ray Powder Diffraction Data for Titanium TiO <sub>2</sub> (Rutile) and TiO <sub>2</sub> (Anatase).	19

## LIST OF ILLUSTRATIONS

<u>Figure</u>		<u>PAGE</u>
1	Components in Ultra High Vacuum for ISS/SIMS Surface Analysis	21
2	Survey Photoelectron Spectrum of Ti-6Al-4V Alloy Treated by the Phosphate-Fluoride Process	22
3	Oxygen, Titanium and Carbon Regions of the Photoelectron Spectrum of Ti-6Al-4V treated as shown	23
4	Degradation of TiO <sub>2</sub> with Time Due to Electron Beam Heating as shown by Ti Soft X-Ray Appearance Potential Spectra (ref. 12)	24
5	ISS/SIMS Data from as received Ti-6Al-4V Alloy	25
6	Scanning Electron Micrographs of Alkaline Cleaned Ti-6Al-4V Alloy (marker in $\mu\text{m}$ .)	26
7	ISS/SIMS Data from Alkaline Cleaned Ti-6Al-4V Alloy	27
8	Comparison of Scanning Electron Micrographs of Alkaline Cleaned and Alkaline Etched Ti-6Al-4V	28
9	ISS/SIMS Data From Alkaline Etched (Turco 5578) Ti-6Al-4V	29
10	Scanning Electron Micrographs of Phosphate-Fluoride Treated Ti-6Al-4V Alloy. (marker in $\mu\text{m}$ .)	30
11	ISS/SIMS Data from Phosphate-Fluoride Treated Ti-6Al-4V	31
12	Scanning Electron Micrographs of Autoclaved Phosphate Fluoride Treated Ti-6Al-4V. (marker in $\mu\text{m}$ .)	32
13	ISS/SIMS Data from Autoclaved phosphate-Fluoride Treated Ti-6Al-4V	33
14	Scanning Electron Micrographs of Pasa-Jell 107 Treated Ti-6Al-4V Alloy. (marker in $\mu\text{m}$ .)	34
15	ISS/SIMS Data From Pasa-Jell 107 Treated Ti-6Al-4V Alloy	35
16	Scanning Electron Micrographs of Autoclaved Pasa-Jell 107 Treated Ti-6Al-4V. (marker in $\mu\text{m}$ .)	36
17	ISS/SIMS Data from Autoclaved Pasa-Jell Treated Ti-6Al-4V	37
18	Scanning Electron Micrographs of Vought Abrasive Slurry Treatment of Ti-6Al-4V. (marker in $\mu\text{m}$ .)	38

<u>Figure</u>		<u>PAGE</u>
19	ISS/SIMS Data From Vought Abrasive Slurry Treatment of Ti-6Al-4V	39
20	X-ray Diffractometer Traces of Chemically Etched Side of VAST Surface (Top) and Combination Chemical/Mechanical VAST Etched Surface (bottom) with Corresponding Scanning Electron Micrographs	40

### LIST OF TABLES

<u>TABLE</u>		
1	Summary of Surface Chemistry Techniques (ISS/SIMS)	4

## SECTION I

### INTRODUCTION

The need for lighter, higher strength structures makes it necessary to develop new classes of materials such as composite and adhesively bonded materials. The surface composition and morphology of these metals, compounds and alloys are extremely important in their fabrication and use. The surface composition of many alloys bears little resemblance to the bulk composition. Segregation during heat treatment can result in surface properties (either deleterious or beneficial) far different from the bulk. Chemical treatments can selectively dissolve some components and not others, which results in large changes in composition and properties. Chemical treatments also can leave behind impurities both as combined and adsorbed species. McDevitt and coworkers have shown such phenomena for several aluminum alloys which were subjected to numerous chemical treatments (ref. 1, 2). These aluminum alloys have been used extensively for secondary structures and are projected for use as primary load bearing members. Unfortunately, aluminum alloys, primarily because of low melting points, do not possess the properties necessary for advanced aerospace structures. Therefore Titanium and its alloys because of light weight, thermal stability and high strength have been under development for aerospace applications. Conventional methods of joining titanium alloys such as welding, bolting and rivetting are used, but just as in Aluminum alloys, the advantages of adhesive bonding make it necessary to develop surface treatments for Ti which produce adhesive joints which are strong and durable. Adhesive joints possess a more uniform stress distribution, are lighter, and are better sealed against corrosion than conventional joints.

The requirement of operation in excess of 250°C applications places a severe burden on both the adhesive and the interfacial region between the adhesive and adherend in the joint. Joint failures under adverse conditions have often been blamed on the adhesive but a recent study (ref. 3) suggests that the adherend surface may likely be the cause of failure in many cases. Surface

treatments have been developed to give optimum bonding surfaces which produce durable bonded joints. This involves not only creating a surface of the proper structure and roughness, but also of the correct chemistry to insure long time use under deleterious conditions. It is therefore necessary to be able to determine elemental composition and morphology for a surface following each surface treatment. Certain treatments may be used to strip off the natural oxide in preparation for a treatment such as anodization, where the natural oxide is replaced by the anodic oxide of carefully controlled thickness. Other treatments etch the surface to provide mechanical (hook and latch) attachment of adhesive to adherend. Still others replace the natural oxide with a chemically formed/oxide or conversion coating which is both bondable and durable.

In this work, we are investigating the effect on the surface of several surface treatments on Ti (commercially pure), Ti-6Al-4V, and Ti 8 Mn. We are also looking at various structural aspects of titanium oxides formed on the above materials. Finally, we are determining effects of some surface treatments on multiphase titanium alloys containing four or more elements. In this report we begin by reporting results on Ti-6Al-4V subjected to several commercial treatments. Although the chemistry of the Ti-6Al-4V surface has been investigated by others, we will attempt to summarize results to date and to show new data utilizing the combination ISS/SIMS method.

## SECTION II EXPERIMENTAL

The samples of Ti-6Al-4V alloy which had been subjected to standard commercial surface treatments were obtained from Edward Arvay, Non-metallic Materials Division, Air Force Materials Laboratory. Mr. Arvay was furnished these samples by Vought Systems Division, LTV Aerospace Corporation. The samples were analyzed without any further preparation by ISS/SIMS. This dual method uses a low energy ion beam (1-3 KeV) to probe the surface. The ISS (Ion Scattering Spectrometry) method measures the energy loss when the probing ion scatters from the outermost atom layer at the surface. The SIMS (Secondary Ion Mass Spectrometry) technique measures the mass spectrum of the sputtered ions which are removed from the surface by the primary ion beam. Table I shows the operating parameters and advantages of both techniques. The two methods are very complementary, with the weakness of one usually the strength of the other. The equipment used on this work is the ISS Model 520 (3M Co., St. Paul, Minn.) to which was added the UTI (UTHE Technology International, Sunnyvale, CA) model 100 C quadrupole mass analyzer as shown in Figure 1. Installation of a simple three element energy filter on the front of the quadrupole mass analyzer allowed recording of +SIMS data.

Primary ion beams at 2500V of  $^{20}\text{Ne}^+$ ,  $^4\text{He}^+$  and  $^3\text{He}^+$  were used to scatter and sputter surface ions for analysis. Appendix A and B contain ion scattering and mass information to aid the reader in interpretation of spectra.

The scanning electron microscope used in this work was the Quikscan (Coates and Welter Corp., Sunnyvale, CA) operated by William Lampert of this laboratory. Some SEM photographs were also obtained at the University of Dayton Research Institute by Dr. Richard Harmer using a JEOL JSMU-3 scanning electron microscope. Photoelectron spectra were obtained by Dr. William Moddeman of the University of Dayton Research Institute. X-ray diffractometer scans were obtained with a Philips Electronics vertical diffractometer using step scanning and digital processing and plotting of diffraction

TABLE I. SUMMARY OF SURFACE CHEMISTRY TECHNIQUES (ISS/SIMS)  
TECHNIQUE

PARAMETER	ION SCATTERING SPECTROSCOPY ISS	SECONDARY ION MASS SPECTROSCOPY SIMS
Principle	Elastic Binary Collision with Surface Ion	Sputtering of Surface Atoms by Ion Beam
Probe	~1-3 KeV Ions	~1-3 KeV Ions
Signal	Ion Current vs Energy	Ion Current vs Mass
Applicable Elements	$Z \geq 3$	All (if pos & neg SIMS)
Sensitivity, General	High	Variable
Sensitivity, Low Z	Low	High
Resolution (Spectral)	Low	High
Spectral Shift Information on Chemical Combination	Possible, but Generally No	No
Quantitative Anal Influence of Operating Conditions and Matrix	No	In Some Cases Usually No
Isotopic Analysis	Yes	Probably No
B Beam Induced Surface Changes	No	Maybe w/Similar Standards
	Yes, in Principle But Generally No Because of Resolution Limits	Yes
	No	No

data. James S. Solomon of the University of Dayton Research Institute performed the x-ray diffraction work. Procedures for commercial surface treatments for titanium and titanium alloys as outlined partially in reference 4 are listed as follows:

VOUGHT ABRASIVE SURFACE TREATMENT (VAST)

1. Wipe surface with methyl ethyl ketone
2. Alkaline Clean - Turco 5578, 5 oz/gal
3. Rinse with D.I. water at room temperature
4. VAST process 2%  $H_2SiF_6$  5-10 minutes  
Rinse tap water spray at room temperature
5. Rinse tap water spray at room temperature
6. Immerse 1 minute in solution 5%  $HNO_3$   
(optional depending on titanium alloy)
7. Rinse D.I. water at room temperature
8. Air Dry

Pasa Jell 107 (P-J)

1. -3. Same as above.
4. Acid Etch - 580 parts/wgt 70%  $HNO_3$   
80 Parts/wgt 50% HF  
1340 parts/wgt D.I. water  
4 minutes removes .0005 inch/surface
5. Rinse with D.I. water at room temperature
6. Pasa-Jell 107 -757 MI Pasa-Jell 107-C7  
1627 MI 70%  $HNO_3$   
229 gms  
1400 ml D.I. water  
Dilute 1:1 with D.I. water  
12 minutes at room temperature
7. Spray rinse D.I. water at room temperature
8. Hot D.I. water rinse 150°F for 2 minutes
9. Air Dry

Phosphate-Fluoride (PhF)

1. -5. Same as Pasa-Jell 107
6. Phosphate-Fluoride Treatment
  - Tri-Sodium Phosphate 100 grams
  - Potassium Fluoride 32 grams
  - Hydrofluoric Acid (52%) 33 grams
  - D.I. water, Dilute to 2 liters
  - 2-3 minutes at room temperature
7. Spray rinse D.I. water at room temperature
8. Hot D.I. water rinse 150°F, 15 minutes
9. Spray rinse D.I. water at room temperature
10. Air Dry

Alkaline Etch - Turco 5578

1. -3. Same as above
4. Etch - Turco 5578 4 pounds per gal
  - 180°F for 10 minutes
5. Spray rinse D.I. water at room temperature
6. Hot D.I. water rinse at 150°F for 2 minutes
7. Air Dry

Alkaline Clean (ALK)

1. Hand wipe with methyl-ethyl-ketone
2. Etch for four minutes in 10:1 HNO<sub>3</sub>:HF
3. Immerse in alkaline solution 20 minutes at 250°F solution
  - composition 600 grams NaOH
  - dilute to one liter
4. Rinse in tap water
5. De oxidize 15 seconds in 10:1 HNO<sub>3</sub>:HF
6. Rinse in tap water
7. Rinse in de-ionized water
8. Blow dry with clean air

## SECTION III

### SUMMARY OF EARLIER WORK

The chemistry of Ti-6Al-4V surfaces after commercial treatment has been mentioned in several reports (refs. 3, 4, 5, 6) and SEM photographs for selected treatments have been shown for the alloy in numerous reports (refs. 3, 4, 5, 7, 8, 9). The chemistry of the surface has been most often deduced by photoelectron spectroscopy, also known as ESCA (Electron Spectroscopy for Chemical Analysis). Photoelectron spectroscopy is a very useful analysis tool because in addition to providing elemental analysis, information on how the ions are combined is also available from the fine features of the spectra. Photoelectron spectroscopy has in the past been considered somewhat slower than methods like Auger electron spectroscopy, but computer control and data acquisition as well as other instrumental improvements have speeded analysis by electron spectroscopy. Because it uses a low energy x-ray beam to excite photoelectrons, this technique is somewhat less destructive than methods using an electron beam. Figure 2 shows a survey spectrum of Ti-6Al-4V alloy which was given the phosphate fluoride treatment. Hamilton and Lyerly have examined such spectra carefully and determined how several elements are bonded (ref. 3) on alkaline and phosphate-fluoride treated specimens. For instance, they find that phosphorus exists not as phosphate but as phosphide in the phosphate-fluoride treated specimen. Lively (ref. 4) has shown elemental information for a variety of surface treatments, both chemical and thermal. Generally, Lively does not report all of the elements observed in Figure 2, but as can be seen, whether an element is reported or ignored largely depends on how much the data are expanded and where the cut-off is established concerning reporting an element present. Detailed examination of electron spectra such as in Figure 3 reveals numerous areas of interest. In spectra from the solvent cleaned specimen three components are seen in the Ti 2p lines indicating that photoelectrons are being emitted not only from the oxide, but also from the metal beneath the natural oxide on the surface. Optical measurements on titanium indicate a thickness of 23 Å (ref. 10) of oxide on pure titanium. The Ti 2p  $3/2$  line was arbitrarily assigned an intensity value of 1.00 in each spectrum and then all other lines are compared to Ti 2p. The spectra indicate that the surface treatment influences high temperature behavior and

that there are reactions taking place on the surface which cannot easily be interpreted. Later work on Titanium and Ti alloys will include detailed photoelectron spectra.

Soft x-ray Appearance Potential Spectroscopy (SXRAPS) is another useful tool for determining how an element is combined at the surface (ref. 11). In this laboratory we have reported SXRAPS experiments on Ti c.p., Ti-6Al-4V and Ti-8Mn (ref. 12). The method is useful for extremely stable materials but can cause reduction of oxide species as shown in Figure 4 from ref. 12. Here we see that with time the titanium spectrum changes from that representative of  $TiO_2$  to a reduced species. This reduction is due to surface heating from the electron beam. Some suggestions are given for minimizing this heating by improving sensitivity and decreasing target beam loading (ref. 12). In such a system, the basically simple SXRAPS method should prove very useful and will be used in later phases of this work. Very recent results with a sensitive SXRAPS system using a silicon barrier detector were obtained on titanium using only 150 uA beam current (ref. 13).

Many other surface characterization tools have been utilized by earlier investigators, such as Auger Electron Spectroscopy (refs. 4, 5) Surface Potential Difference (refs. 3, 5) Ellipsometry (ref. 5) and Differential Scanning Calorimetry (ref. 3). Selected area electron diffraction patterns were obtained for oxides removed from Ti-6Al-4V (refs. 3, 5).

SECTION IV  
RESULTS AND DISCUSSION

Ti-6Al-4V Alloy

Ti-6Al-4V is an alpha-beta type alloy. The alpha phase crystallizes in a hexagonally close packed array and the beta phase is body centered cubic. The beta phase is the high temperature form and exists in equilibrium with the alpha phase at room temperature. The alloy is anisotropic and the alpha phase exhibits the property of becoming extinct when viewed under the crossed polars of a polarizing microscope. Patches on the surface became alternately light then dark upon rotation of the polars. Many etches, particularly those which are acidic, selectively etch the alpha phase leaving the beta phase standing out in relief.

Effect of Surface Treatments on Ti-6Al-4V As Received.

The spectral data from the as received alloy which was given no treatment except for degreasing, show only slight differences from the bulk. This is much different from aluminum alloys (ref. 1, 2) where surface compositions of as received rolled sheet showed little resemblance to bulk values. Figure 5 shows ISS/SIMS data from Ti-6Al-4V (as received). The ISS spectra are very sensitive to changes in oxygen/titanium stoichiometry and indicates that the alloy is covered with a  $\text{TiO}_2$  coating. Little information on the alloying elements Al and V is given in ISS spectra of titanium alloys because these elements are located on the tails of Ti and O. In addition, titanium is one of several elements which exhibit severe low energy tailing apparently due to non-binary scattering. The secondary ion mass spectrum does not suffer these limitations as can be seen in Figure 5 where alloying element as well as impurity element lines are visible. In addition, fingerprint spectra in the form of lines at  $\text{TiO}^+$  (and other Ti-O combinations) are characteristic of  $\text{TiO}_2$  at the surface. The line at atomic mass 65 is stronger than calculated on the basis of  $^{49}\text{Ti}^{16}\text{O}$ , particularly on fresh surfaces. This added intensity is due to a second line at the same nominal mass due to  $^{48}\text{Ti}^{16}\text{O}^1\text{H}$ . Hydrogen and Hydroxy/ion are also seen on these surfaces. It cannot be proven whether molecular combinations such as  $\text{TiO}^+$  and  $\text{TiOH}^+$  exist on the surface or if they are formed in a plasma above the surface.

### Alkaline Clean

The alkaline cleaning treatment as enumerated earlier does not disrupt or roughen the surface of the alloy as seen in Figure 6, two scanning electron micrographs of two magnifications. As indicated earlier, the white phase is the B phase according to many investigators. SIMS data as shown in Figure 7 indicate a reduction of aluminum, magnesium and calcium and increased concentration of potassium at the surface. The commercial alkaline etch using Turco 5578 produces a far different surface as will be shown later. Electron diffraction patterns (ref. 4) indicate that the  $\text{TiO}_2$  exists as rutile, the most thermodynamically stable form of  $\text{TiO}_2$ .

### Alkaline Etch

The alkaline etch using Turco 5578 produces much greater etching of the surface as seen in the comparison of Figure 8. It also apparently selectively etches the alloy to expose a vanadium rich phase as shown by + SIMS data of Figure 9 where  $^{51}\text{V}$  is easily compared to  $^{50}\text{Ti}$ . Since the abundance of  $^{50}\text{Ti}$  is about the same order of magnitude as the vanadium content, (if the secondary ion yield is approximately equal for titanium and vanadium) then the vanadium concentration can be easily calculated. This vanadium enhancement is similar to that seen in the Pasa Jell surface reported later.

### Phosphate-Fluoride

The phosphate fluoride treatment roughens the surface only slightly as seen in Figure 10, but the chemistry is significantly changed as indicated by the ISS/SIMS data in Figure 11. Aluminum is nearly totally depleted at the surface and the sodium and calcium present indicate that this oxide is nearly like a sponge for ions of the correct size. It has been reported (ref. 3, 4) that the phosphate-fluoride treatment forms a homogeneous oxide of the anatase structure, which is less stable thermodynamically but has a simpler, more random structure. Perhaps the anatase structure is stabilized by  $\text{Ca}^+$ ,  $\text{Na}^+$  and perhaps other ions not sensitive to + SIMS. The phosphate-fluoride treatment gives an average thickness of oxide of about  $200 \text{ \AA}$  on Ti-6Al-4V (ref. 5). It was found that under certain conditions this anatase structure

converted to rutile and it was felt to be the cause for poor bond durability with time (ref. 3). In an effort to stabilize the anatase phase, attempts were made to incorporate various ions into the lattice (ref. 7). Heat is known to cause transformation of anatase to rutile (ref. 4).

Autoclaving the phosphate-fluoride treated specimen does not seem to change its surface morphology as seen in Figure 12 but the chemistry is significantly changed as seen by ISS/SIMS data in Figure 13. Note the loss of most of the  $\text{Na}^+$  and  $\text{Ca}^+$  and the return to original concentrations of  $\text{Al}^+$ . Note also that although  $\text{F}^+$  still exists in the Phl' autoclave specimen,  $\text{HF}^+$  has completely disappeared.

#### Pasa-Jell 107

Pasa-Jell 107 treatment also does not drastically change the surface roughness as seen in Figure 14. However early ISS traces such as that shown in Figure 15 indicate roughness differences on an atomic scale which shows up as less well defined scattering peaks compared to a "smooth" surface. Note that P-J leaves the surface somewhat depleted of aluminum and with slightly more (about two times) vanadium than in the bulk alloy. Sodium content is very high.

Autoclaving the pasa-jell 107 surface seems to uncover or at least make the B phase more obvious in the SEM photos of Figure 16. The chemistry is changed slightly with aluminum enhanced at the surface and fluorine also becomes much more visible as shown in Figure 17. It has been reported that pasa-jell 107 leaves the oxide in a mixed amorphous-rutile mixture which when heated to  $350^\circ\text{F}$ , transforms to mixed amorphous, anatase and rutile. When heated to  $600^\circ\text{F}$  the mixture stabilizes in the rutile form (ref. 4).

#### VAST

The Vought Abrasive Surface Treatment is a method which combines grit impact and chemical treatment to provide a stable, active bonding surface. It has been reported (ref. 4) that the benefits are derived from a combination of simultaneous oxide removal, roughening, and selective etching of the alloy. A

unique chemical state of oxygen and nitrogen was found on the surface of VAST treated specimens which was not present after any of the other surface treatments (ref. 4). Electron diffraction patterns on oxides removed by anodically electropolishing the alloy show anatase to be present, transforming to mixed anatase and rutile at 350<sup>o</sup>F. The SEM photographs (Figure 18) show the surface to be greatly roughened by the combination mechanical and chemical etching. Phase distinction is not evident in agreement with earlier work (ref. 4). The ion scattering spectrum as seen in Figure 19 is weak and peaks poorly defined undoubtedly due to the rough surface. The secondary ion mass spectrum shows a great deal of sodium to be present. Silicon, apparently from the H<sub>2</sub>SiF<sub>6</sub> used in the VAST process, is clearly visible in this data.

Not only does the VAST surface show a roughened surface, but x-ray diffraction patterns show also that the lattice is greatly disturbed. This result was rather surprising since the copper K radiation at 1.54 Å<sup>o</sup> penetrates tens of thousands of angstroms and is hardly considered to be a surface tool. X-ray diffractometer traces are shown for both sides of the VAST sample in Figure 20. At the top is shown the SEM photo and diffractometer trace for the side of the specimen exposed only to the chemical etches. This surface and diffraction pattern is very similar to data observed on surfaces only chemically treated. At the bottom is shown the SEM photo and diffractometer trace for the side of the specimen exposed to both chemical and mechanical etching. The peak broadening is very obvious and indicates significant lattice strain in the titanium apparently caused by very high local stresses imparted by impact of slurry particles on the surface. Appendix C shows x-ray powder diffraction data along with other physical property data for the readers convenience (ref. 14). All of the other specimens mentioned in this report were subjected to x-ray diffraction analysis. Except for minor intensity differences caused by preferred orientation, they all were very similar and showed no evidence of the strained lattice seen in the VAST treated specimen.

## SECTION V CONCLUSIONS

The combination ISS/SIMS technique is very useful for determining changes in surfaces due to different chemical and mechanical treatments. SIMS is especially sensitive to many of the elements usually found in chemical treatments and complements the other techniques such as Auger and photoelectron spectroscopies which have previously been used on titanium and its alloys. Changes in chemistry due to autoclaving are easily followed by SIMS. Such results may indicate impurity stabilization of the anatase phase in some treatments as well as the mechanism for destabilization at rather low temperatures. The x-ray diffraction results showed severe lattice strain not only on the surface but apparently extending into the specimen on mechanically disturbed surfaces (VAST). Such strained surfaces would not appear to be desirable. The advantages of the process are roughening the surface and producing a new oxide while simultaneously removing the natural oxide. If lattice damage could be annealed, long time durability might be further improved.

## REFERENCES

1. McDevitt, N.T., Baun, W.L., and Solomon, J.S., AFML-TR-7
2. McDevitt, N.T., Baun, W.L., and Solomon, J.S., AFML-TR-7
3. Hamilton, W.C., and Lyerly, G.A., Picatinny Arsenal Report 4185, March 1971
4. Lively, G.W., AFML-TR-73-270, Part I; January 1974, Part II; August 1975
5. Smith, T., and Kaelble, D.H., AFML-TR-74-73, June 1974
6. Wegman, R.F., Ross, M.C., Slota, S.A., Duda, E.S., Picatinny Arsenal Report 4186, September 1971
7. Hamilton, W.C., and Lyerly, G.A., Picatinny Arsenal Report 4362, June 1972
8. Bush, T.A., Counts, M.E., Ward, T.C., and Wightman, J.P., Final Report NASA Contract NASI - 10646-14, November 1973
9. Counts, M.E., and Wightman, J.P., Final Report NASA Contract NASI-10646-25, November 1974
10. Andreeva, V., and Shishakov, Zhur. Fiz. Khim. 32, 1671 (1958)
11. Houston, L.E., and Park, R.L., J. Vac. Sci. Technol., 10, 176 (1973)
12. Chamberlain, M.B., and Baun, W.L., AFML-TR-74-175, September 1974
13. Andersson, S., and Nyberg, C., Surf. Sci, 52, 489 (1975)
14. The Powder Data File, Published by ASTM, 1916 Race Street, Philadelphia, Pennsylvania

Appendix A  
Positions of Ion Scattering Peaks  
( $E/E_0$ ) for  $Z = 1 - 50$

ELEMENT			E/E <sub>0</sub> (at $\theta = 90^\circ$ )			
Z	A	A.	<sup>3</sup> He	<sup>4</sup> i	<sup>20</sup> Ne	<sup>40</sup> Ar
1	1.0	H		---		
2	4.0	He	.143	0	---	---
3	6.9	Li	.393	.266	---	---
4	9.0	Be	.500	.385	---	---
5	10.8	B	.565	.459	---	---
6	12.0	C	.600	.500	---	---
7	14.0	N	.647	.555	---	---
8	16.0	O	.684	.600	---	---
9	19.0	F	.727	.652	---	---
10	20.2	Ne	.741	.669	.005	---
11	23.0	Na	.769	.704	.070	---
12	24.3	Mg	.780	.717	.097	---
13	27.0	Al	.800	.742	.149	---
14	28.1	Si	.807	.751	.168	---
15	31.0	P	.824	.771	.216	---
16	32.1	S	.829	.778	.232	---
17	35.5	Cl	.844	.797	.279	---
18	39.9	Ar	.860	.818	.332	---
19	39.1	K	.857	.814	.323	---
20	40.1	Ca	.861	.819	.334	.001
21	45.0	Sc	.875	.837	.385	.059
22	47.9	Ti	.882	.846	.411	.090
23	50.9	V	.889	.854	.436	.120
24	52.0	Cr	.891	.857	.444	.130
25	54.9	Mn	.896	.864	.466	.157
26	55.8	Fe	.898	.866	.472	.165
27	58.9	Co	.903	.873	.493	.191
28	58.7	Ni	.903	.872	.492	.189
29	63.5	Cu	.910	.881	.521	.227
30	65.4	Zn	.912	.885	.532	.241
31	69.7	Ga	.917	.891	.554	.271
32	72.6	Ge	.921	.896	.568	.290
33	74.9	As	.923	.899	.578	.304
34	79.0	Se	.926	.904	.596	.328
35	79.9	Br	.928	.905	.600	.333
36	83.8	Kr	.931	.909	.615	.354
37	85.5	Rb	.932	.911	.621	.363
38	87.6	Sr	.934	.913	.628	.373
39	88.9	Y	.935	.914	.633	.379
40	91.2	Zr	.936	.916	.640	.390
41	92.9	Nb	.937	.917	.646	.398
42	95.9	Mo	.939	.920	.655	.411
43	99	Tc	.941	.922	.664	.424
44	101.1	Ru	.942	.924	.670	.433
45	102.9	Rh	.943	.925	.675	.440
46	106.4	Pd	.945	.928	.684	.454
47	107.9	Ag	.946	.929	.687	.459
48	112.4	Cd	.948	.931	.698	.475
49	114.8	In	.949	.933	.703	.483
50	118.7	Sn	.951	.935	.712	.496

Appendix B  
Relative Abundance of Naturally Occurring  
Isotopes,  $Z = 1 - 44$

B. RELATIVE ABUNDANCES OF NATURALLY OCCURRING ISOTOPES

Z	A	1	2	3	4	5	6	7	8	9	10	11	12	13	14	15	16	17	18	19	20	
1	H	99.9	0.1																			
2	He			100																		
3	Li					7.4	92.6															
4	Be								100													
5	B									18.3	81.7											
6	C											98.9	1.1									
7	N													99.6	0.4							
8	O															99.8	0.04	0.20				
9	F																			100		
10	Ne																					90.9
Z	A	21	22	23	24	25	26	27	28	29	30	31	32	33	34	35	36	37	38	39	40	
10	(Ne)	6.3	8.8																			
11	Na			100																		
12	Mg				78.6	10.1	11.3															
13	Al							100														
14	Si								92.2	4.7	3.1											
15	P											100										
16	S												95.0	0.8	4.2		0.02					
17	Cl															75.5		24.5				
18	Ar																0.34		0.06			99.6
19	K																			93.1	0.01	
20	Ca																					97.0
Z	A	41	42	43	44	45	46	47	48	49	50	51	52	53	54	55	56	57	58	59	60	
19	K	6.9																				
20	Ca		0.6	0.1	2.1		0.03		0.2													
21	Sc					100																
22	Ti						8.0	7.3	74.0	5.5	5.2											
23	V										0.3	99.7										
24	Cr										4.3		83.8	9.6	2.3							
25	Mn															100						
26	Fe																91.7	2.2	0.3			
27	Co																			100		
28	Ni																				67.8	26.2
Z	A	61	62	63	64	65	66	67	68	69	70	71	72	73	74	75	76	77	78	79	80	
28	(Ni)	1.2	3.6		1.2																	
29	Cu			69.1		30.9																
30	Zn				48.9		27.8	4.1	18.6		0.6											
31	Ga									60.5	39.5											
32	Ge										20.5		27.4	7.7	36.7		7.7					
33	As															100						
34	Se														0.9		9.0	7.6	23.5			49.8
35	Br																			50.6		
36	Kr																		0.4			2.3
Z	A	81	82	83	84	85	86	87	88	89	90	91	92	93	94	95	96	97	98	99	100	
34	(Se)		9.2																			
35	(Br)	49.4																				
36	(Kr)		11.5	11.5	56.9		17.4															
37	Rb					72.2		27.8														
38	Sr				0.6		9.9	7.0	82.5													
39	Y									100												
40	Zr										51.5	11.2	17.1		17.4		2.8					
41	Nb													100								
42	Mo												15.9		9.1	15.7	18.5	9.5	23.7			9.6
43	Tc	DOES NOT OCCUR NATURALLY																				
44	Ru															5.6			1.9	12.7	12.6	

Appendix C  
X-Ray Powder Data for Titanium,  
 $\text{TiO}_2$  (Rutile), and  $\text{TiO}_2$  (Anatase)

C.

5-0682 MINOR CORRECTION

d	2.74	2.76	2.74	2.557	Ti			
I/I <sub>1</sub>	100	30	26	30	TITANIUM			
Rad. CuK $\alpha_1$	A 1.5405	Filter Ni	d Å	I/I <sub>1</sub>	hkl	d Å	I/I <sub>1</sub>	hkl
Dia.	Cut off	Coll.	2.557	30	010	0.885	9	302
I/I <sub>1</sub> G. C. DIFFRACTOMETER	d corr. Å	d corr. Å	2.342	26	002			
Ref. SWANSON AND FUYAT, NBS CIRCULAR 539, Vol. III (1953)			2.244	100	011			
			1.726	19	012			
			1.475	17	110			
Sys. HEXAGONAL	SG D <sub>6h</sub> - P <sub>6</sub> /amc		1.332	16	103			
a 2.950 b <sub>1</sub>	c <sub>1</sub> 4.486 A	C 1.500	1.276	2	200			
a	$\beta$	$\gamma$	1.267	16	112			
Ref. I.B.I.D.		Z 2	1.233	15	201			
			1.1704	2	014			
St	n = #	f <sub>y</sub>	1.1220	2	202			
SV	D <sub>1</sub> 4.503 mp	Color	1.0653	3	014			
Ref. I.B.I.D.			0.9895	6	203			
			.9458	11	211			
			.9175	10	114			
			.8927	4	212			
			.8796	4	015			
			.8636	2	204			
			.8514	4	300			
			.8211	12	213			

SAMPLE FROM NEW JERSEY ZINC CO., PREPARED BY THE IODIDE PROCESS. SPECT. ANAL. : .026 Al; .0125 Fe, Mo; .0088 Mn; .0045 Ni; .00255 Mg; .0028 Cu. X-RAY PATTERN AT 25°C. REPLACES 1-1197, 1-1198

4-0551 MAJOR CORRECTION

d	3.25	1.69	2.49	3.245	Ti <sub>2</sub> O <sub>3</sub>			
I/I <sub>1</sub>	100	50	41	100	TITANIUM TRIOXIDE (ANATASE)			
Rad. CuK $\alpha_1$	A 1.5405	Filter Ni	d Å	I/I <sub>1</sub>	hkl	d Å	I/I <sub>1</sub>	hkl
Dia.	Cut off	Coll.	1.741	14	110	1.7495	4	4 0
I/I <sub>1</sub> G. C. DIFFRACTOMETER	d corr. Å	d corr. Å	2.489	41	101	1.1140	1	410
Ref. SWANSON AND TATGE, J.C. FEL. REPTS. 185 (1952)			2.217	23	211	1.1191	4	222
			2.108	21	111	1.0521	4	300
			2.154	9	210	1.1404	5	411
Sys. TETRAGONAL	SG D <sub>2d</sub> - P4/am*		1.697	50	211	1.1161	4	312
a 3.254 b <sub>1</sub>	c <sub>1</sub> 2.958 A	C 2.715	1.624	16	200	1.1273	3	420
a	$\beta$	$\gamma$	1.470	8	010			122
Ref. I.B.I.D.		Z 4	1.453	6	310	1.1142	2	1 2
			1.370	17	301	1.1071	3	200
St	n = #	f <sub>y</sub>	1.347	-	112	1.0917	3	210
SV	D <sub>1</sub> 1.100 mp	Color	1.305	1	211	1.0902	5	213
Ref. I.B.I.D.			1.243	3	202	1.0815	6	421
			1.218	1	212	1.0705	5	1 2
			1.1704	4	301	1.0637	5	422
						1.0571	1	313
						1.0114	8	211

MINOR CORRECTION. SPECTROGRAPHIC ANALYSIS SHOWS NO IMPURITY GREATER THAN 0.001%. X-RAY PATTERN AT 25°C. FOR 2 HRS. FOLLOWED BY 1 HR. C. H. H. TO REPLACE 1-1272, 2-1074 AND 3-1122 AT 25°C.

4-0477 MINOR CORRECTION

d	3.51	1.89	2.98	3.51	TiO <sub>2</sub>			
I/I <sub>1</sub>	100	33	22	100	TITANIUM DIOXIDE (ANATASE)			
Rad. CuK $\alpha_1$	A 1.5405	Filter Ni	d Å	I/I <sub>1</sub>	hkl	d Å	I/I <sub>1</sub>	hkl
Dia.	Cut off	Coll.	3.51	100	101	1.1869	3	118
I/I <sub>1</sub> G. C. DIFFRACTOMETER	d corr. Å	d corr. Å	2.435	9	103	1.0433	3	321
Ref. SWANSON AND TATGE, J.C. FEL. REPTS. 185 (1952)			2.379	22	104	1.0173	2	100
			2.336	9	112	0.9554	4	216
			1.891	33	200	0.9461	3	400
Sys. TETRAGONAL	SG D <sub>2d</sub> - P4/am*		1.699	21	105	0.9199	2	325
a 3.783 b <sub>1</sub>	c <sub>1</sub> 9.51 A	C 2.51	1.665	19	211	0.8963	3	211
a	$\beta$	$\gamma$	1.498	4	213	0.8879	2	220
Ref. I.B.I.D.		Z 4	1.480	13	204	0.8311	41	327
			1.377	5	116	0.8219	3	415
St	n = #	f <sub>y</sub>	1.337	5	220	0.814	1	309
SV	D <sub>1</sub> 1.899 mp	Color	1.274	10	215	0.796	2	424
Ref. I.B.I.D.			1.250	3	301			
			1.171	2	303			
			1.1609	3	312			

PARKER, Z. KRIST. 23, 1-54 (1923) SPECTROGRAPHIC ANALYSIS SHOWS NO IMPURITY GREATER THAN 0.01%. X-RAY PATTERN AT 26-27°C. TO REPLACE 1-0562, 2-0387, 2-1406, 3-1332

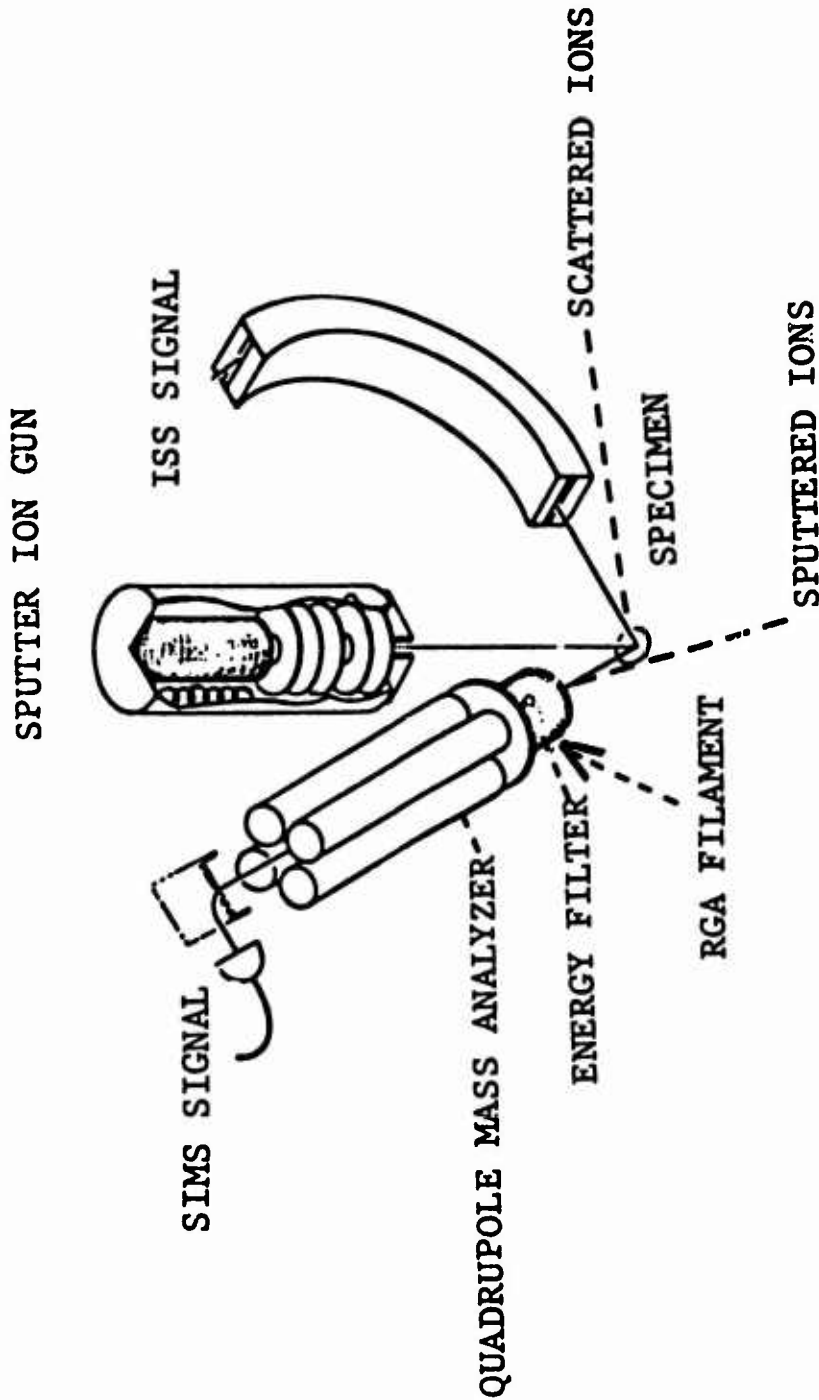


Figure 1. Components in Ultra High Vacuum for ISS/SIMS Surface Analysis

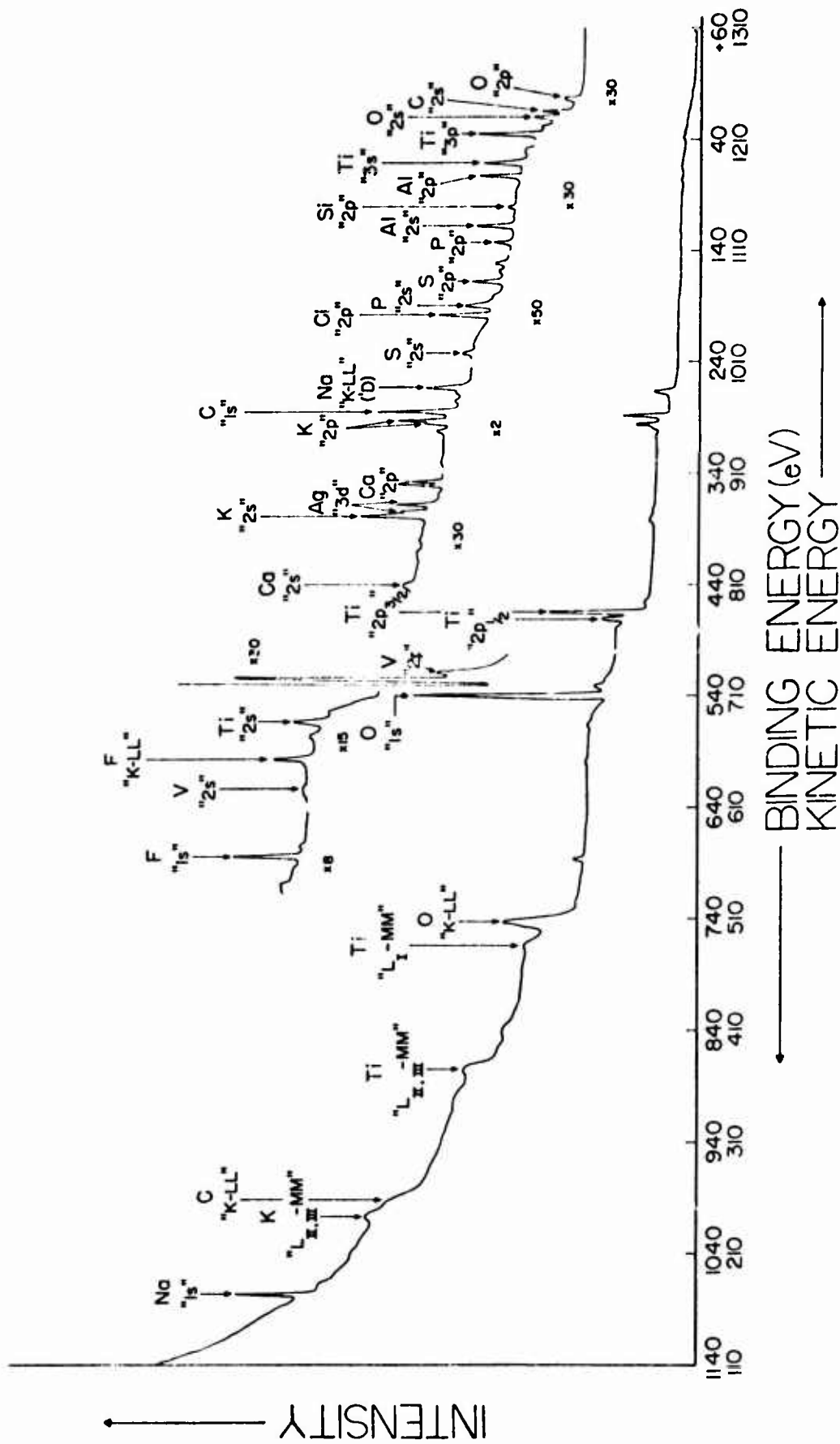


Figure 2. Survey Photoelectron Spectrum of Ti-6Al-4V Alloy Treated by the Pho-phate-Fluoride Process

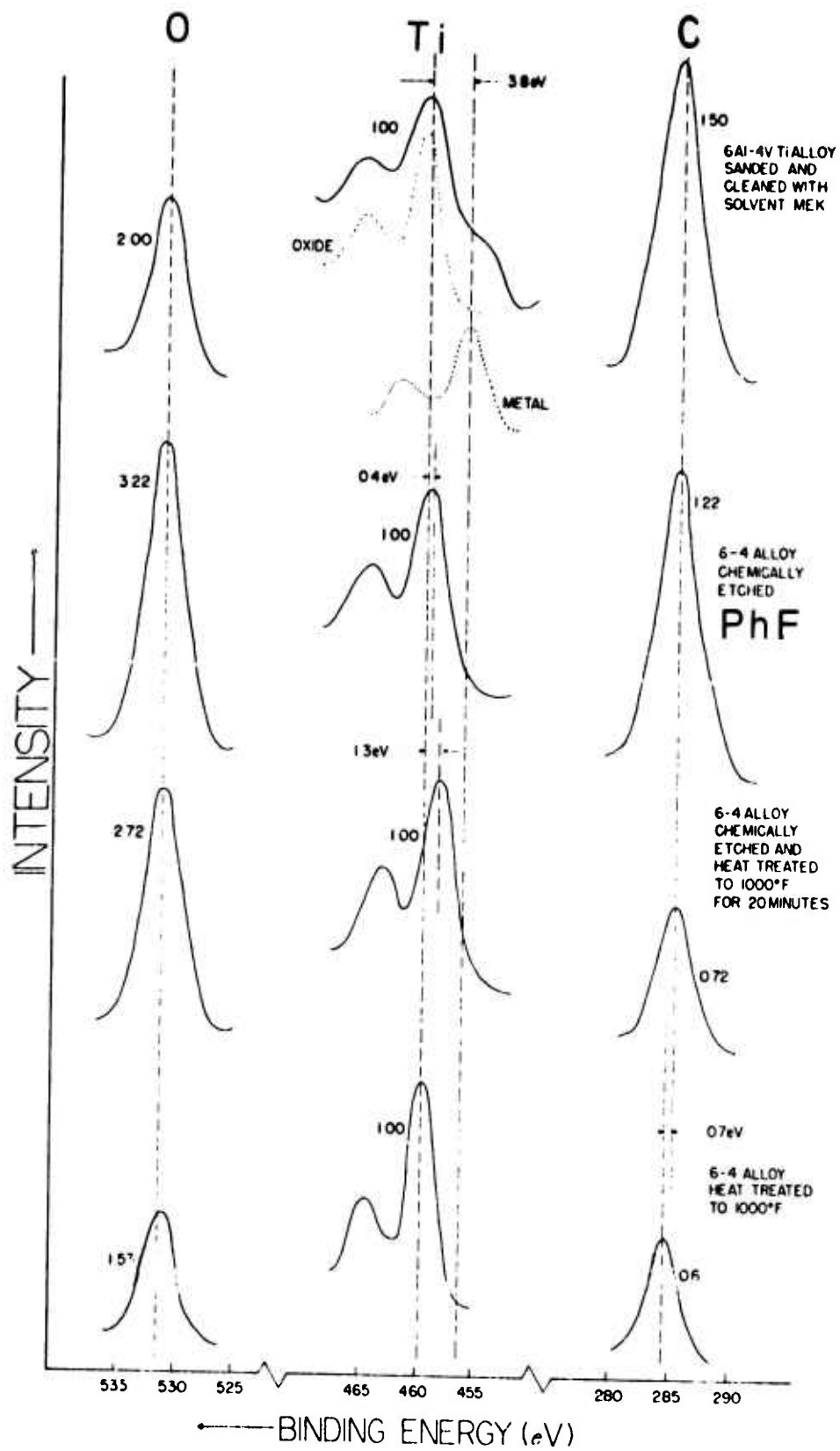


Figure 3.. Oxygen, Titanium and Carbon Regions of the Photoelectron Spectrum of Ti-6Al-4V treated as shown

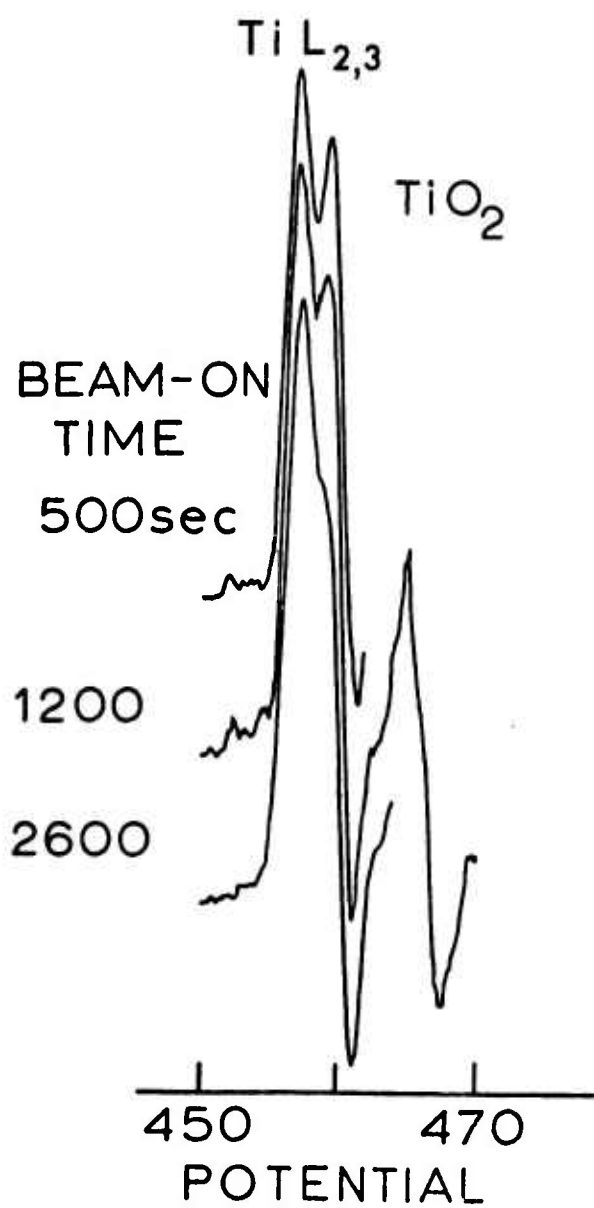


Figure 4.. Degradation of  $\text{TiO}_2$  with Time Due to Electron Beam Heating as shown by Ti Soft X-Ray Appearance Potential Spectra (ref. 12)

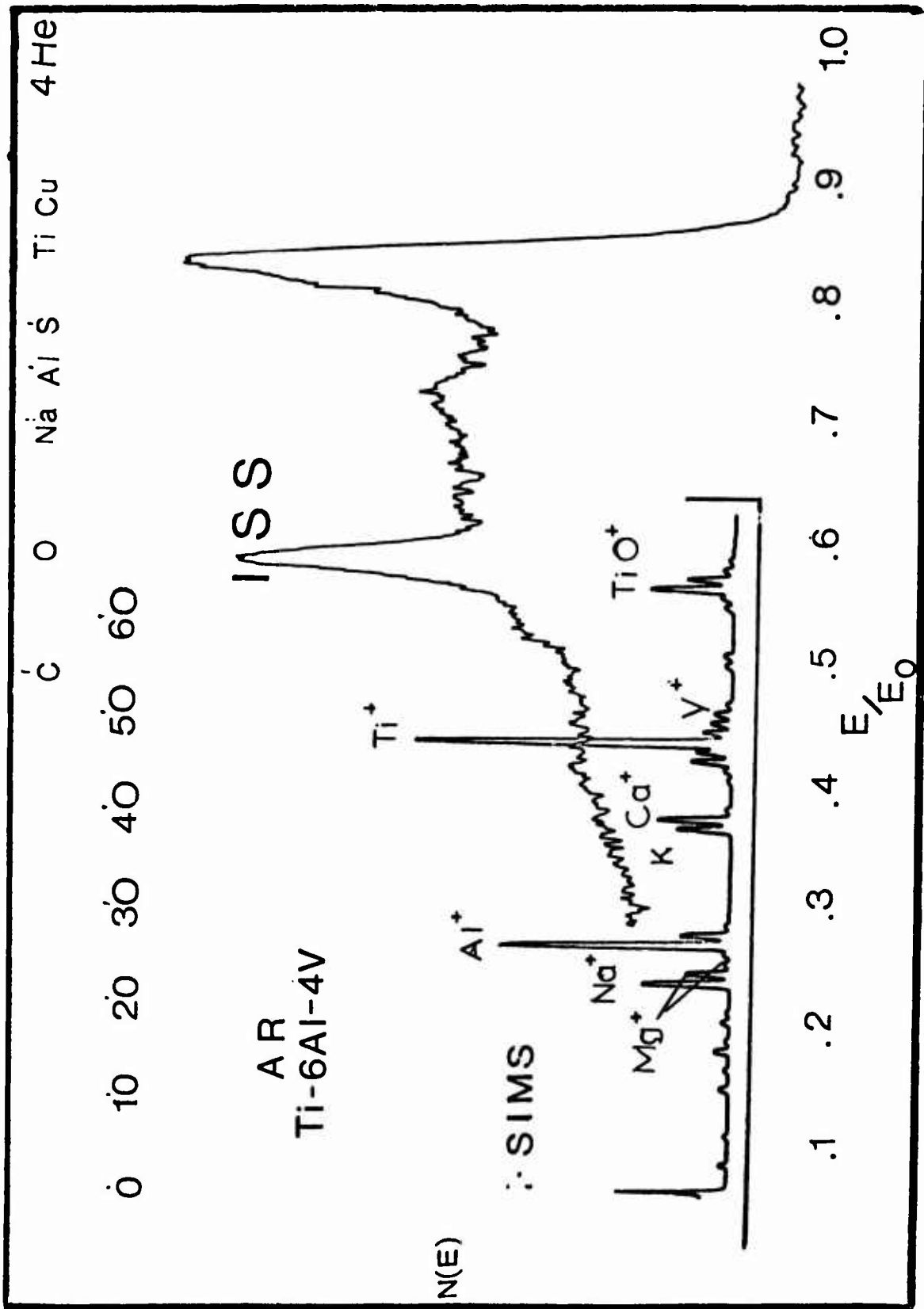


Figure 5. ISS/SIMS Data from as received Ti-6Al-4V Alloy

ALK

Ti-6Al-4V

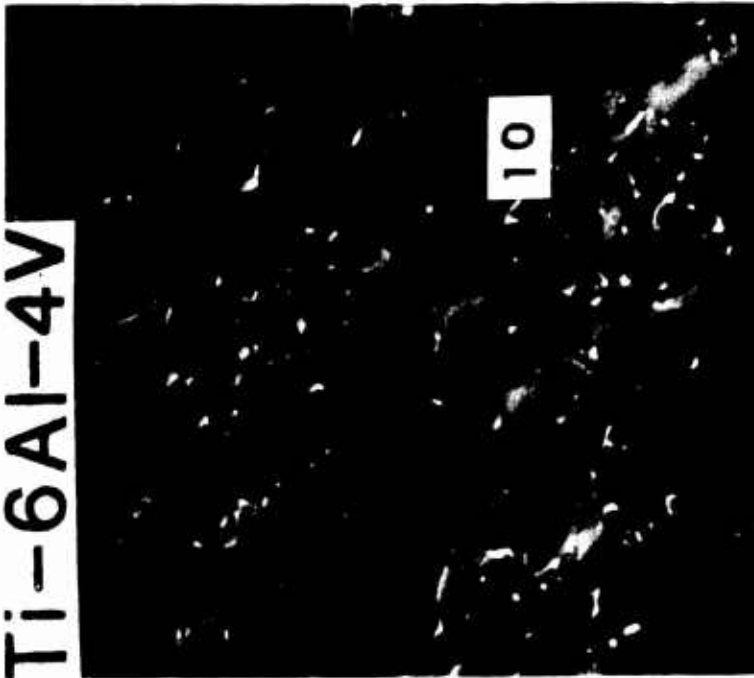


Figure 6. Scanning Electron Micrographs of Alkaline Cleaned Ti-6Al-4V Alloy (marker in  $\mu\text{m}$ .)

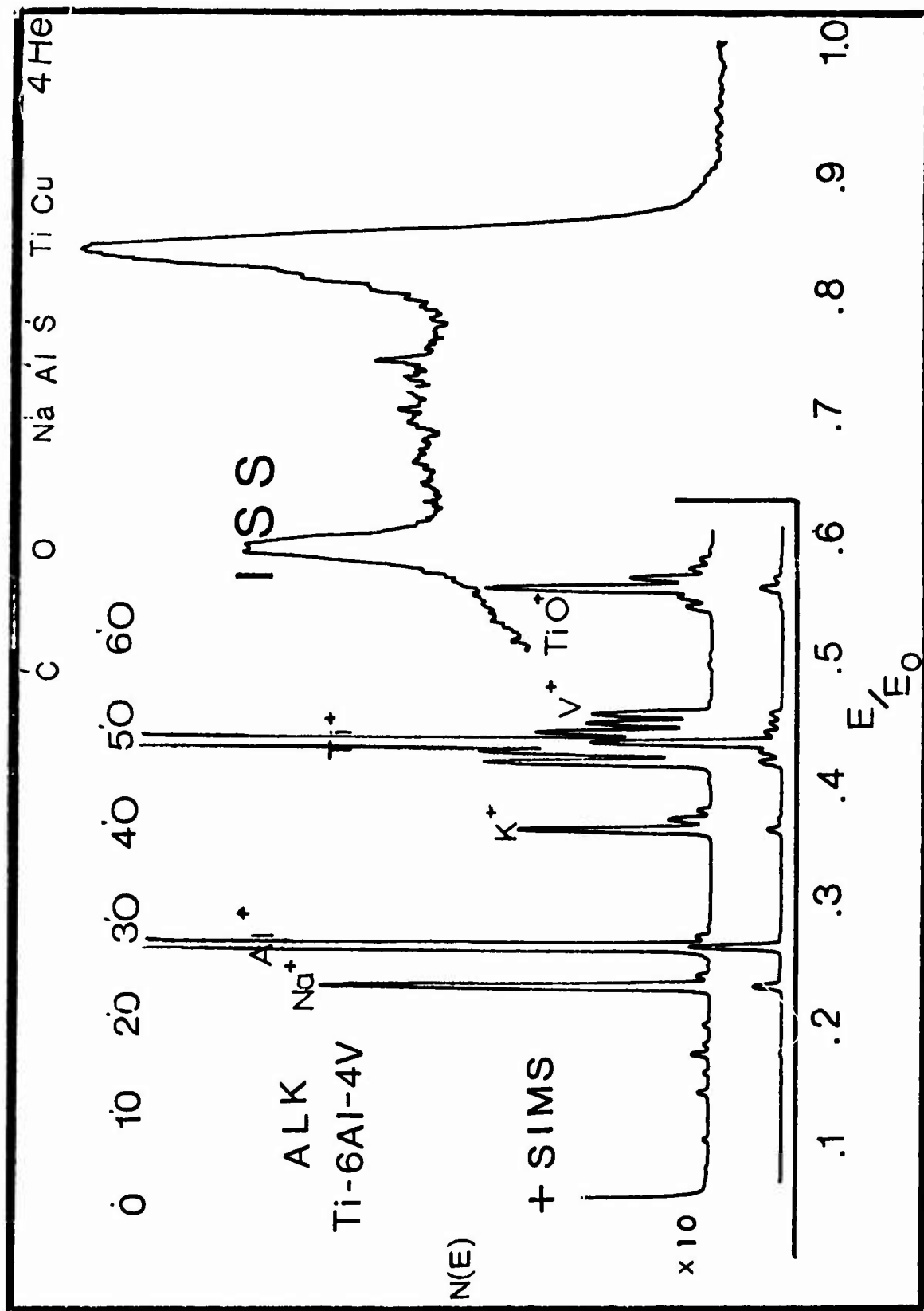


Figure 7. ISS/SIMS Data from Alkali Cleaned Ti-6Al-4V Alloy

ALK (NaOH)



10  $\mu$ m

TUR.55578



2  $\mu$ m



Figure 8. Comparison of Scanning Electron Micrographs of Alkaline Cleaned and Alkaline Etched Ti-6Al-4V

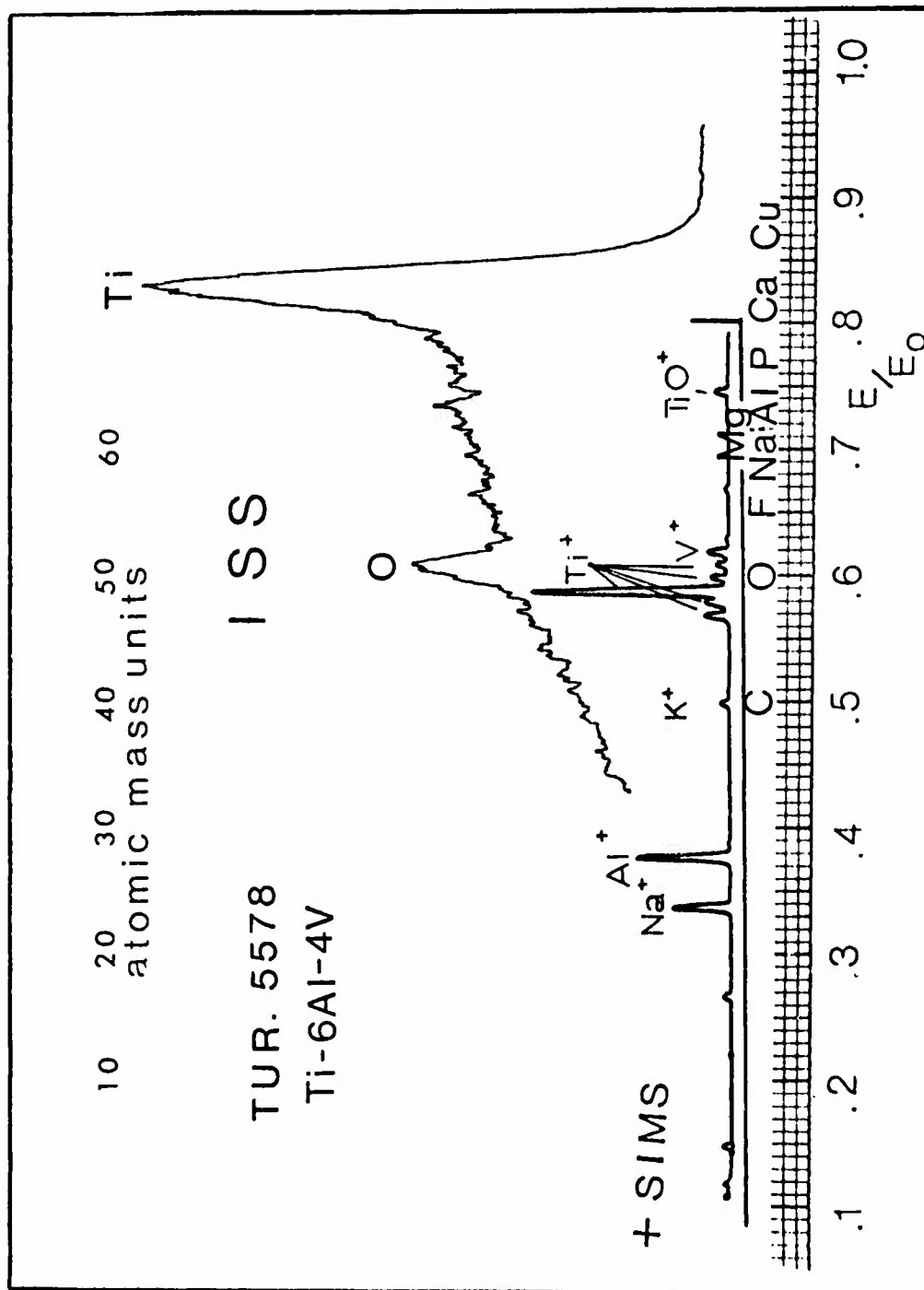


Figure 9. ISS/SIMS Data From Alkaline Etched (Turco 5578) Ti-6Al-4V

Ph F

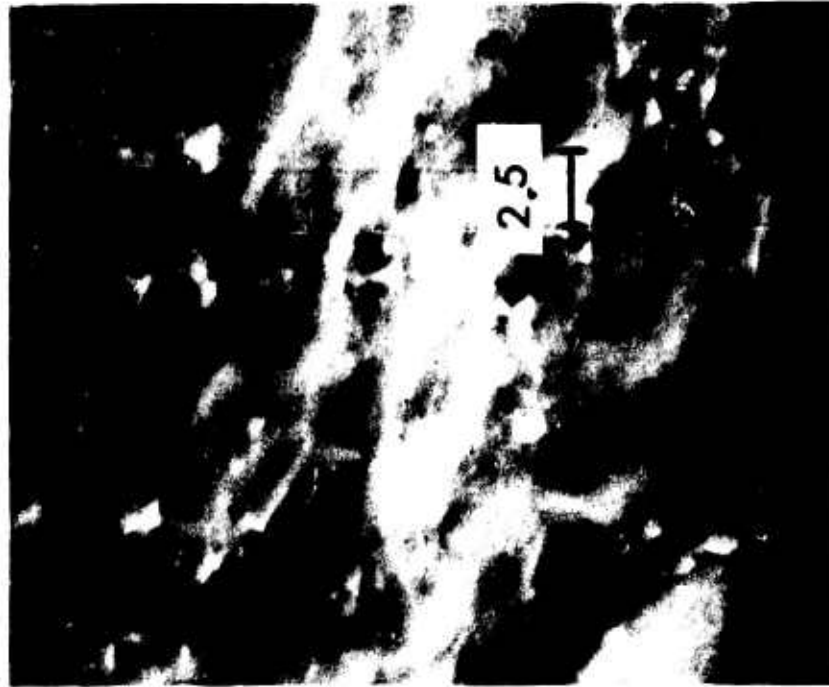
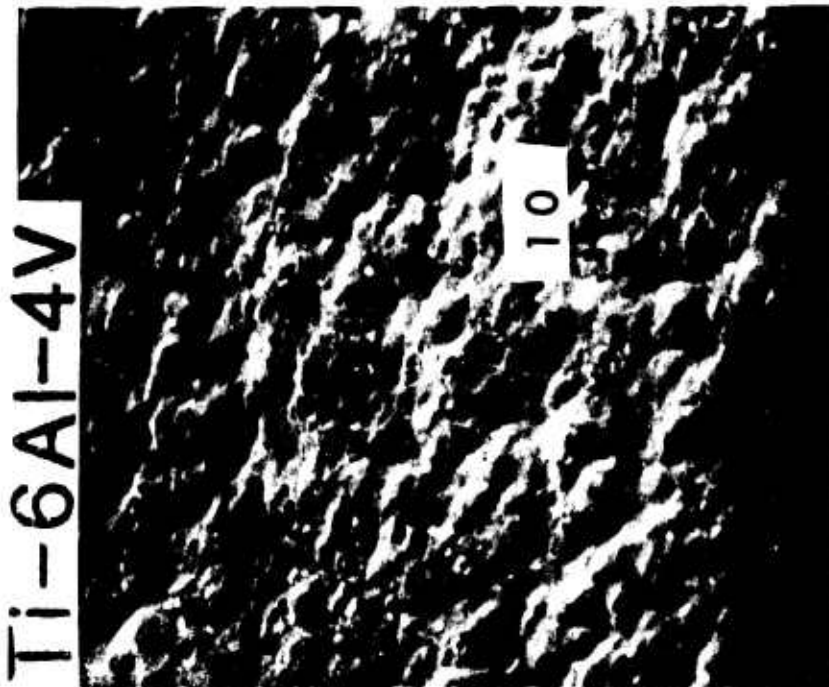


Figure 10. Scanning Electron Micrographs of Phosphate-Fluoride Treated Ti-6Al-4V Alloy. (marker in  $\mu\text{m}$ .)

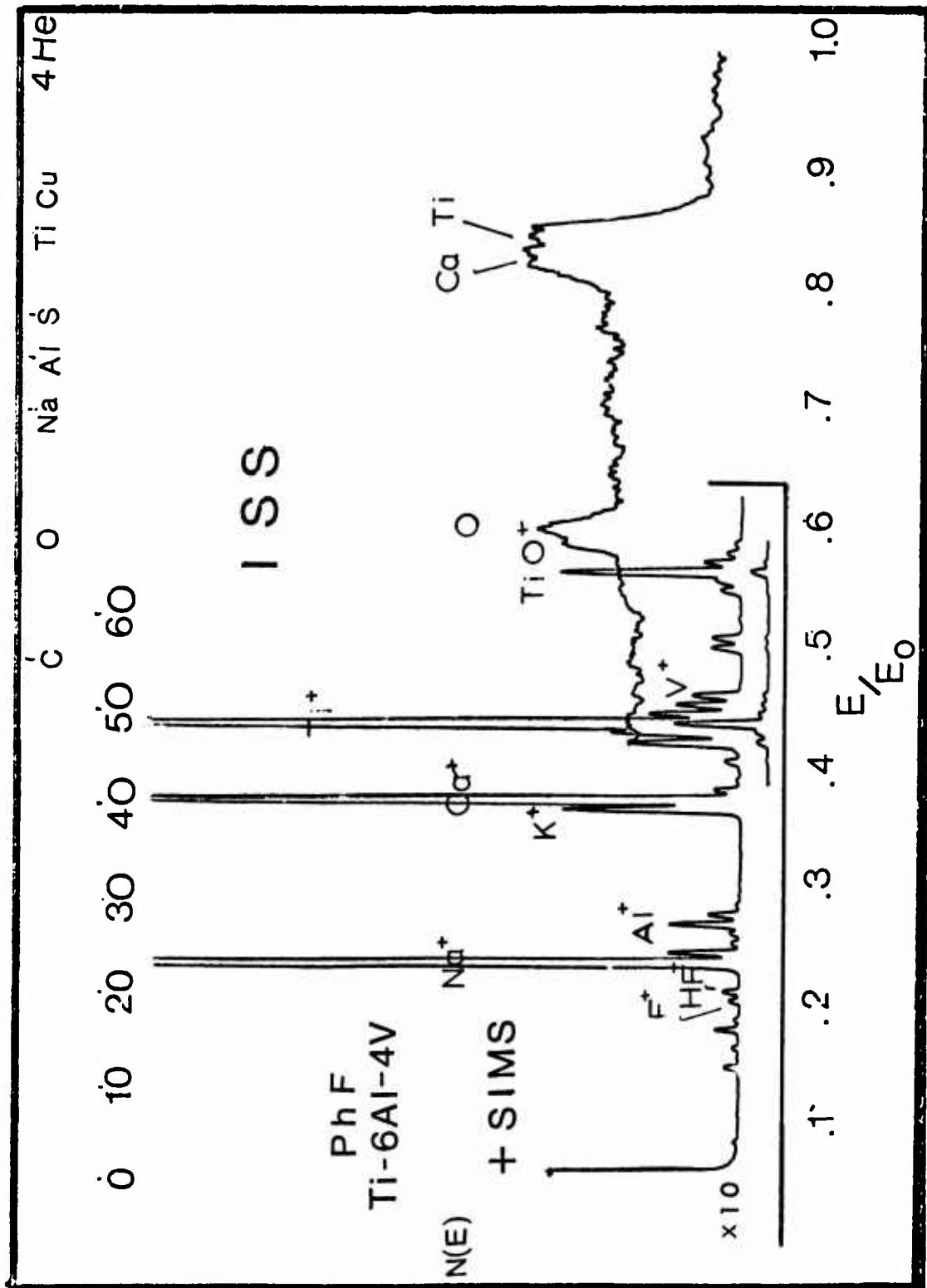


Figure 11. ISS/SIMS Data from Phosphate-Fluoride Treated Ti-6Al-4V

PhF + AUTO

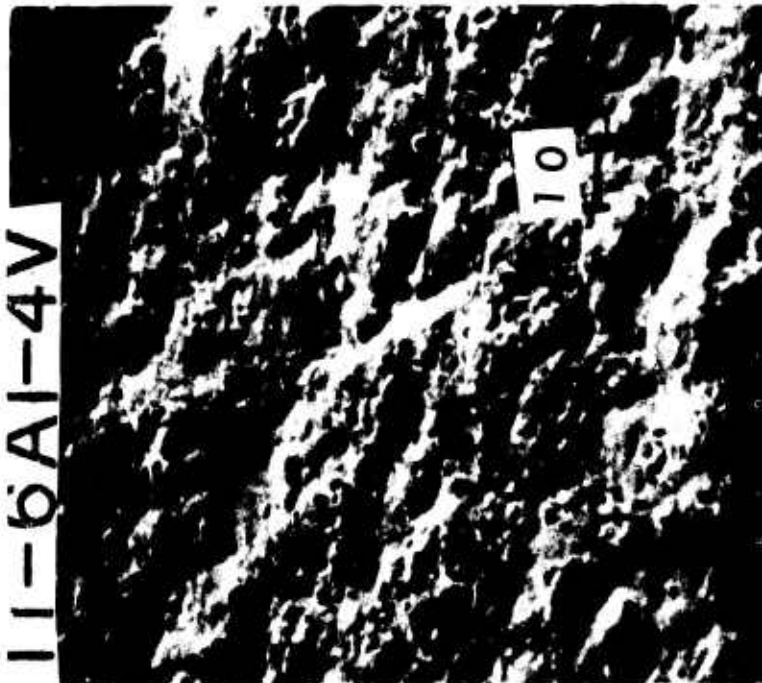


Figure 12. Scanning Electron Micrographs of Autoclaved Phosphate Fluoride Treated Ti-6Al-4V. (marker in  $\mu\text{m}$ .)

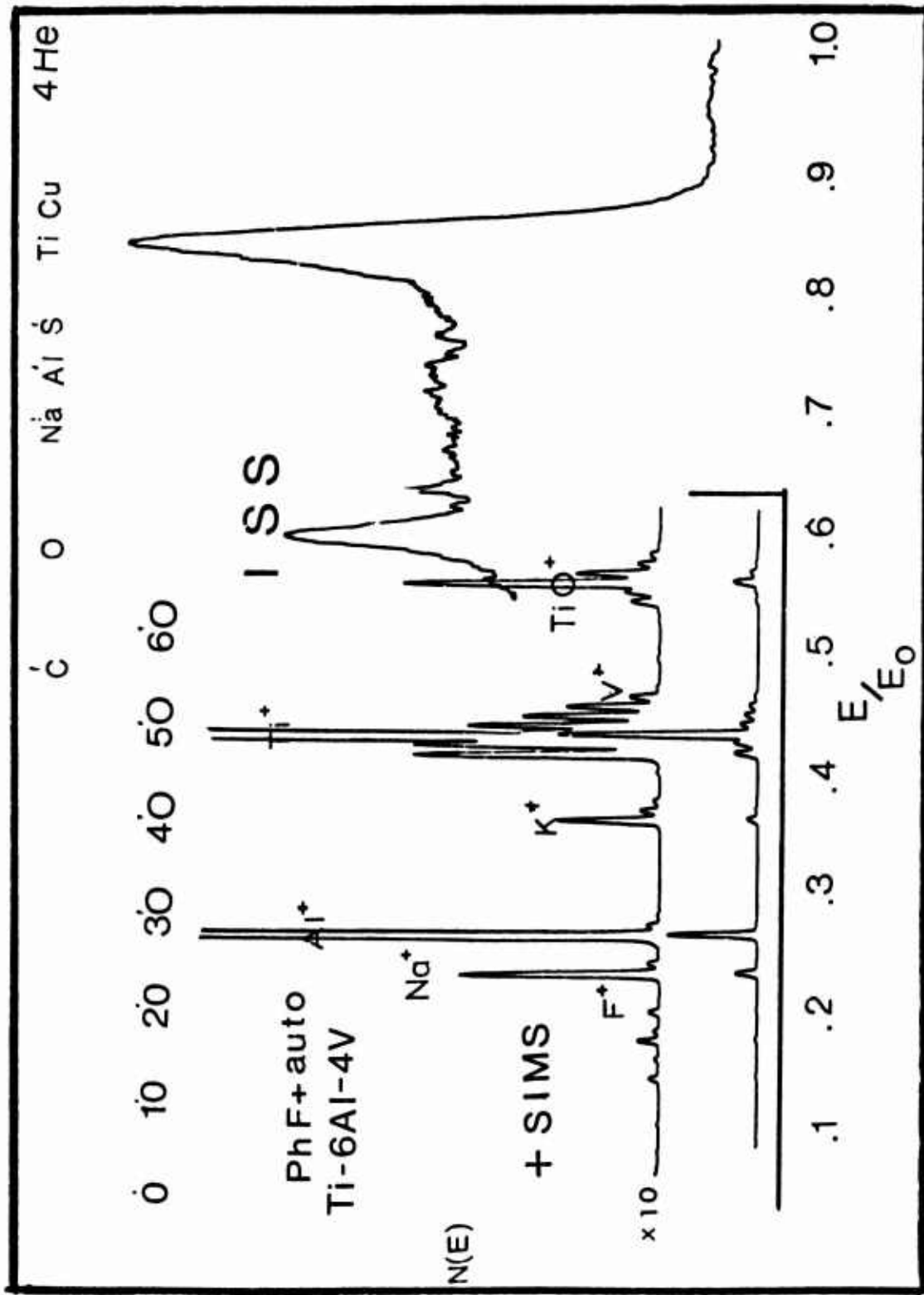


Figure 13 ISS/SIMS Data from Autoclaved phosphate-Fluoride Treated Ti-6Al-4V

P-J

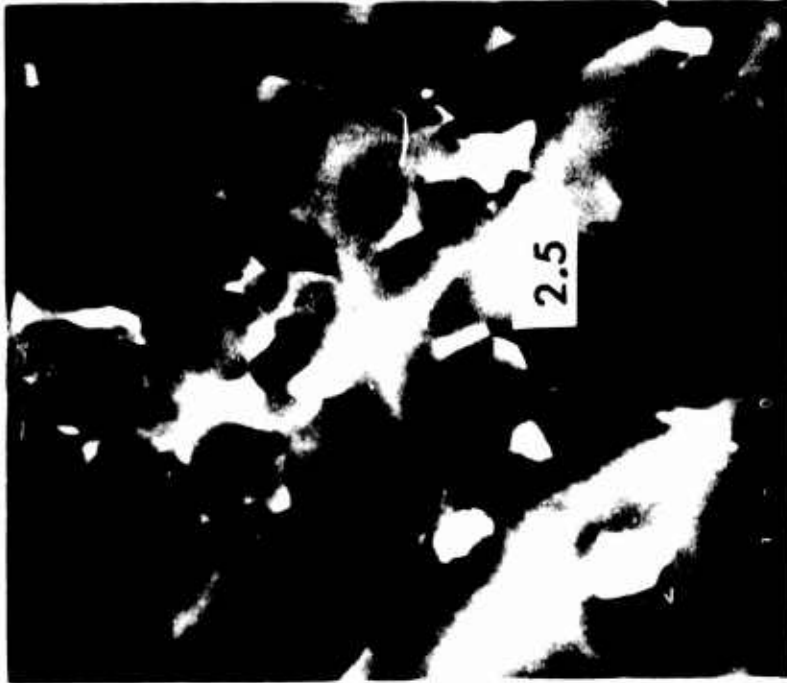


Figure 14 Scanning Electron Micrographs of Pasa-Jell 107 Treated Ti-6Al-4V Alloy. (marker in  $\mu\text{m}$ .)

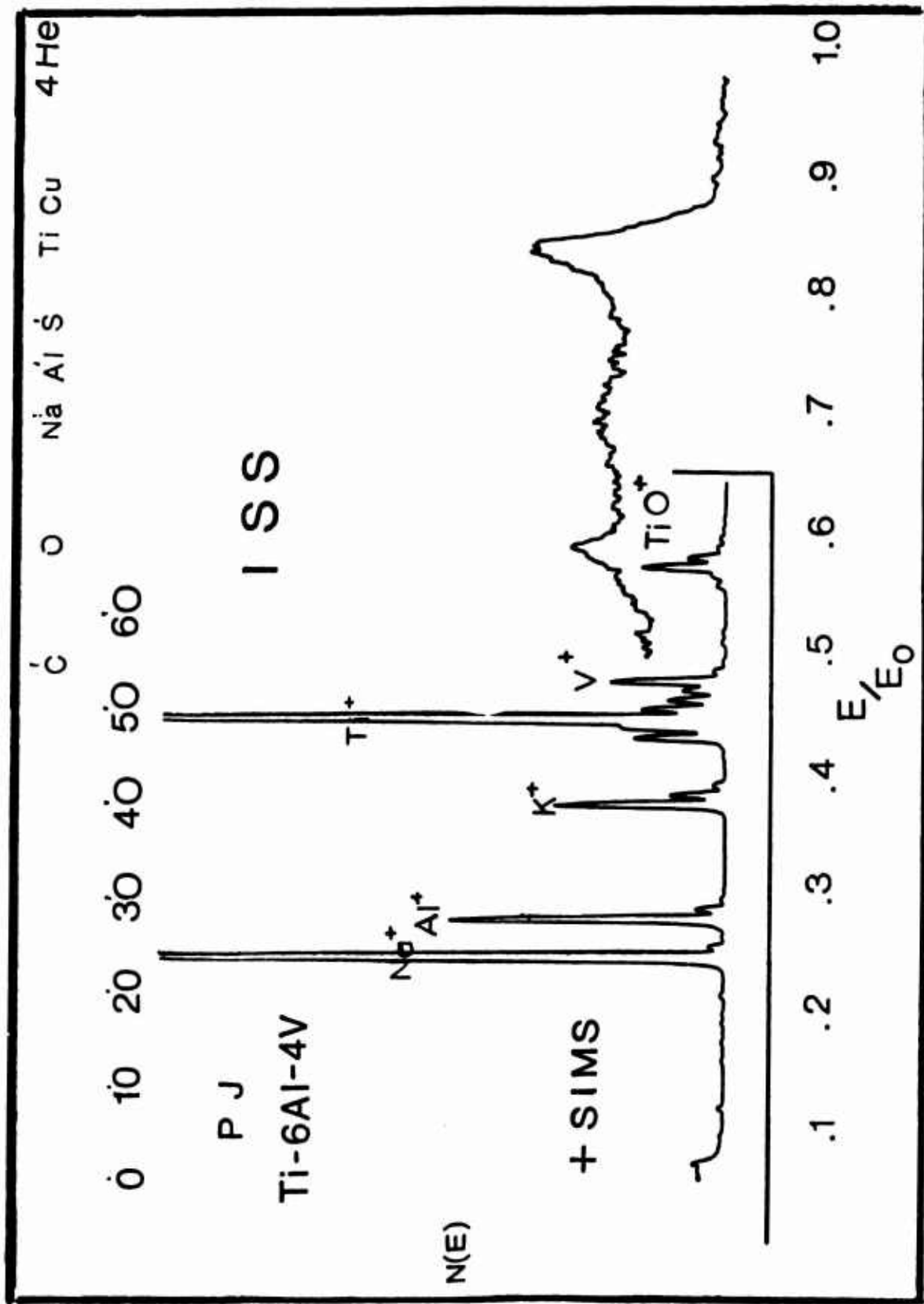


Figure 15 ISS/SIMS Data From Pasa-Jell 107 Treated Ti-6Al-4V Alloy

# P J + AUTO



Figure 16 Scanning Electron Micrographs of Autoclaved Pasa-Jell 107 Treated Ti-6Al-4V. (marker in  $\mu\text{m}$ .)

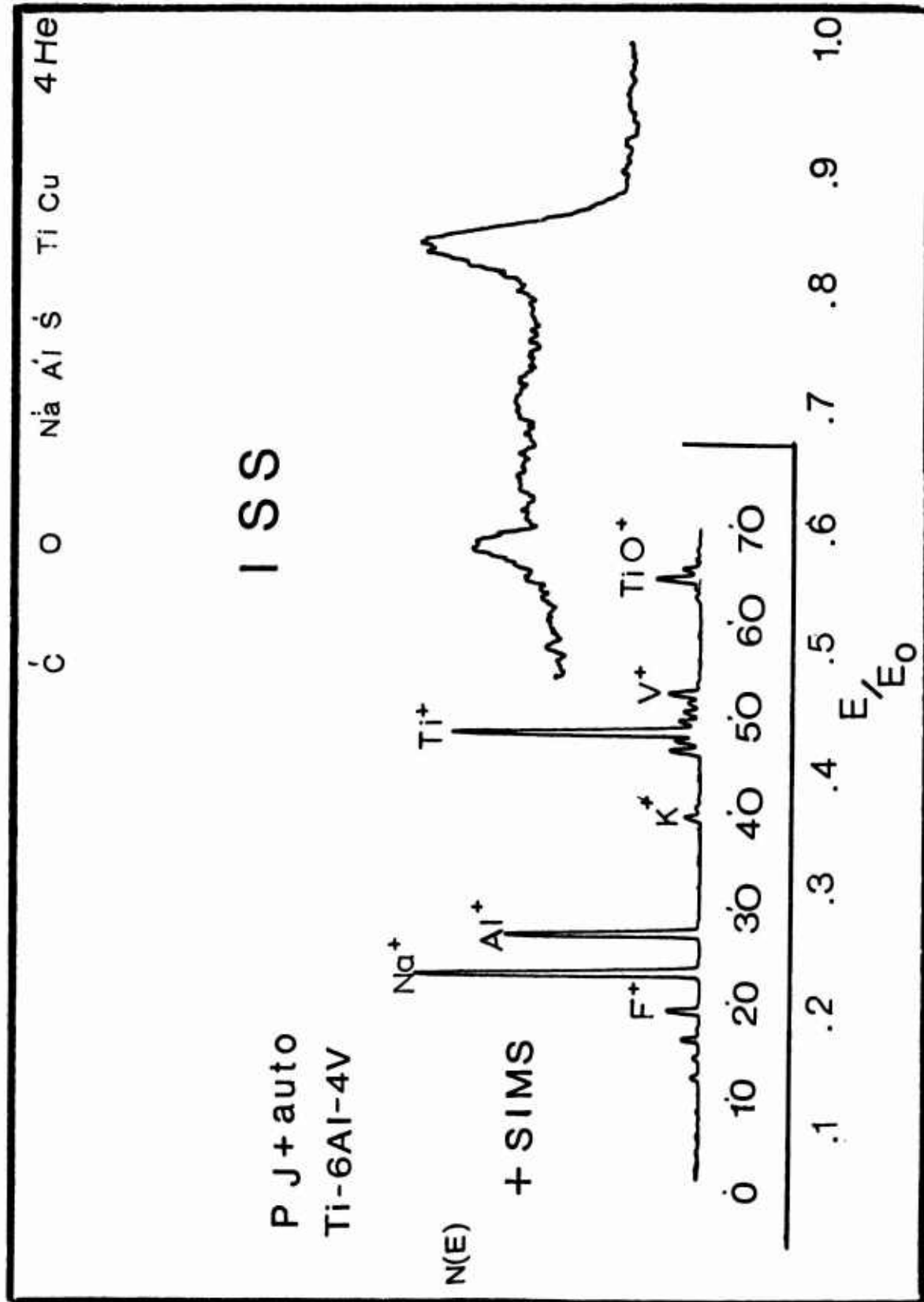


Figure 17. ISS/SIMS Data from Autoclaved Pasa-Jell Treated Ti-6Al-4V

# VAST

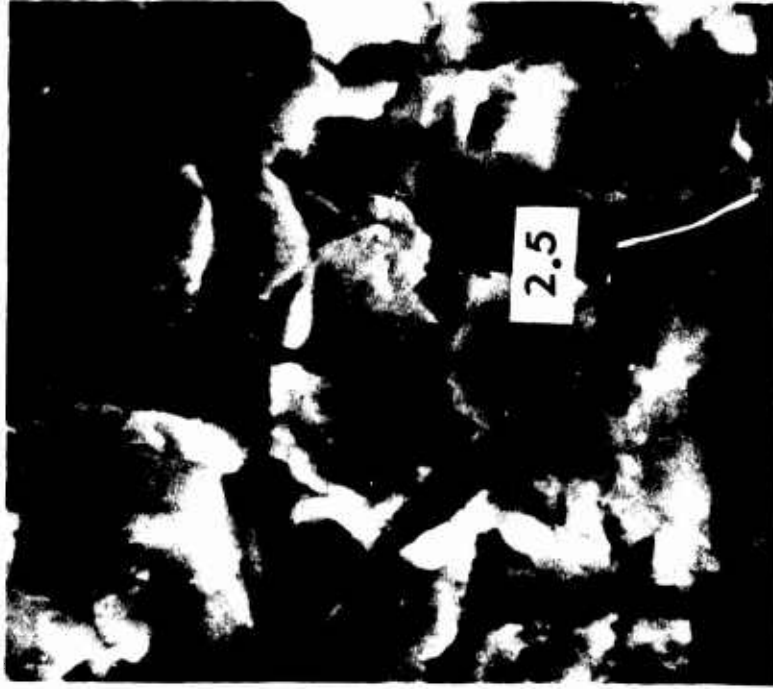


Figure 18 Scanning Electron Micrographs of Vought Abrasive Slurry Treatment of Ti-6Al-4V. (marker in  $\mu\text{m}$ .)

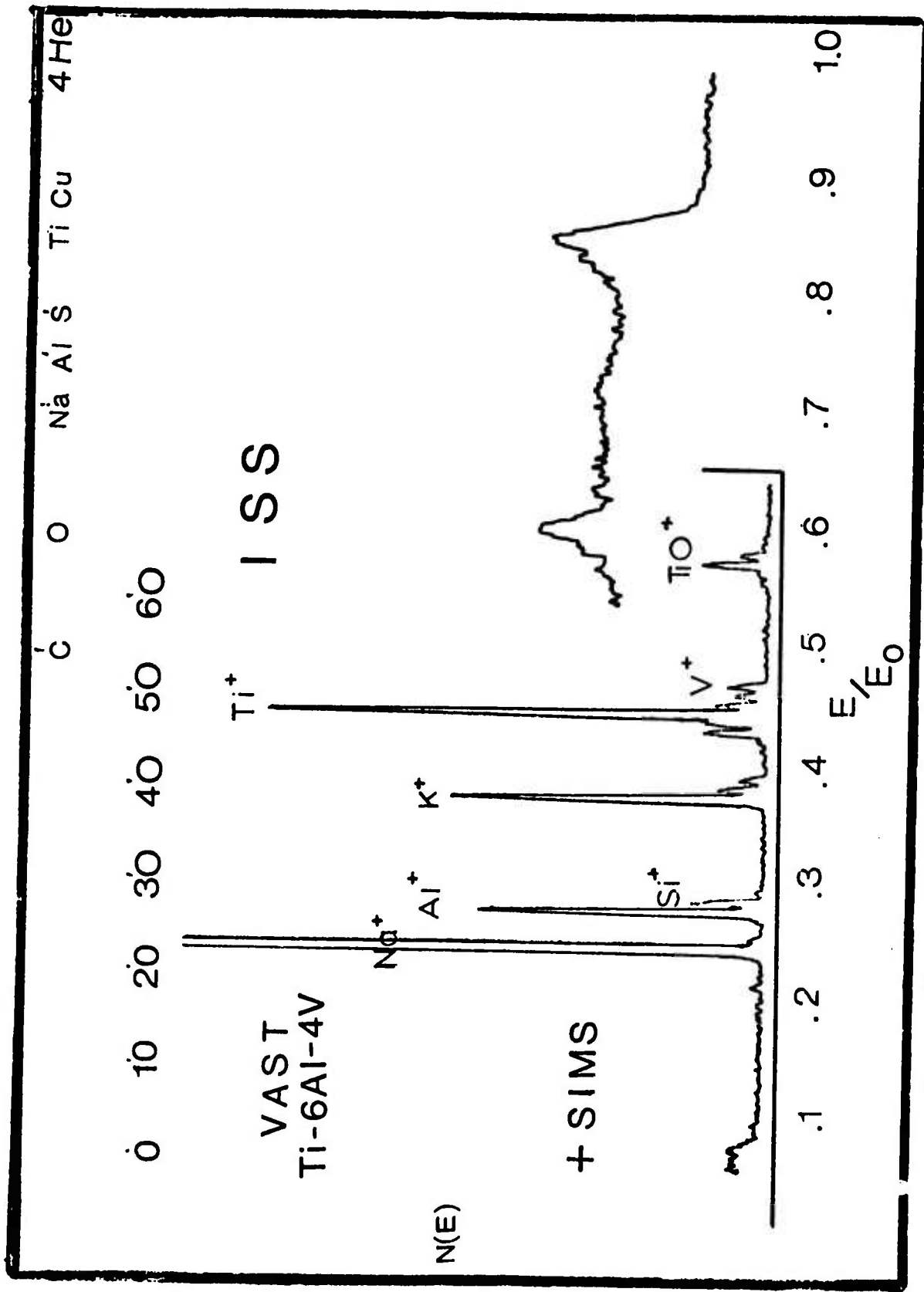


Figure 19. ISS/SIMS Data From Vought Abrasive Slurry Treatment of Ti-6Al-4V

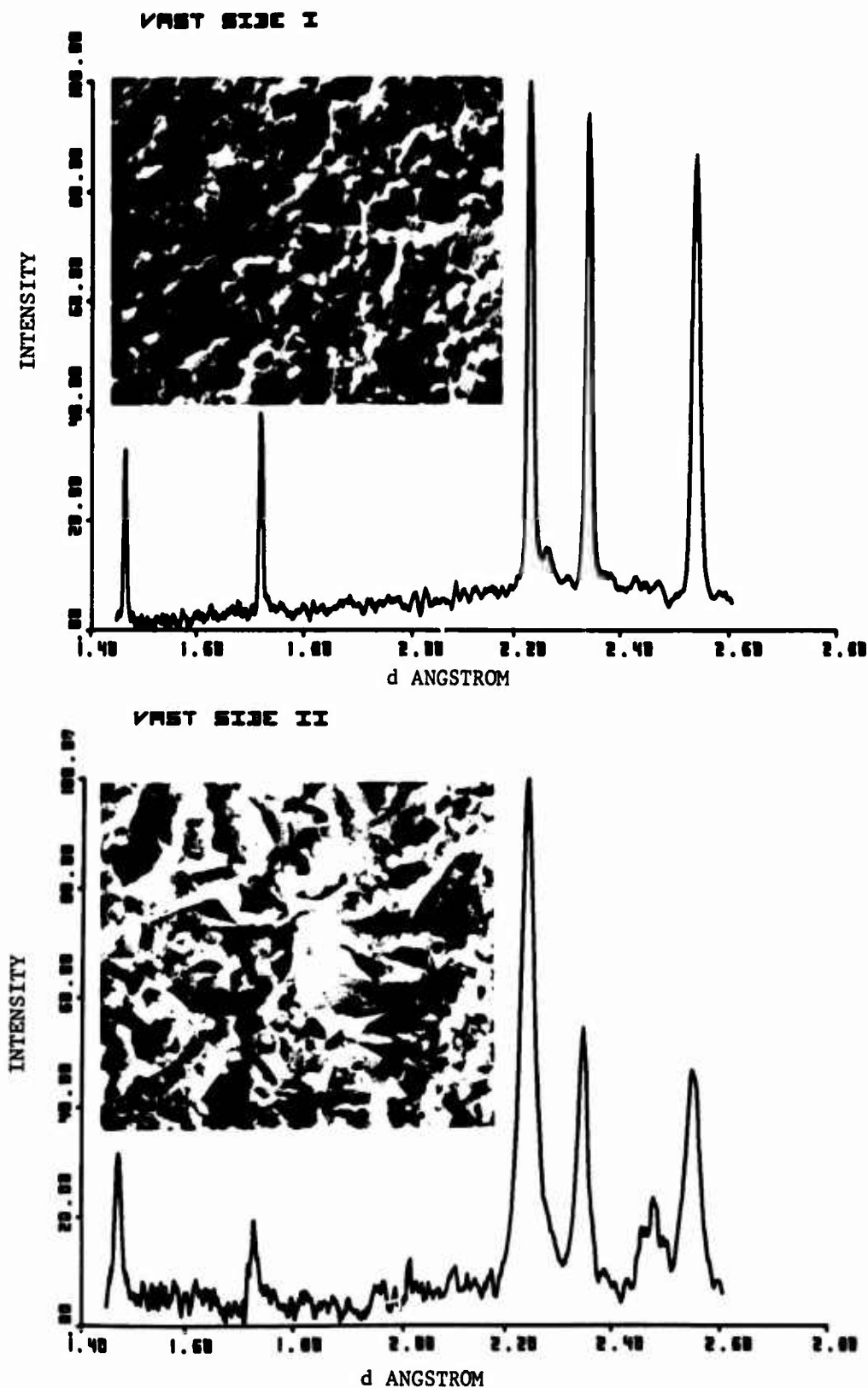


Figure 20. X-ray Diffractometer Traces of Chemically Etched Side of VAST Surface (Top) and Combination Chemical/Mechanical VAST Etched Surface (bottom) with Corresponding Scanning Electron Micrographs